



# Comparison of the effects of epidermal growth factor mesenchymal stem cell and silver sulfadiazine on burn stasis zone

Ömer Kürklü, Sinan Soylu

Department of General Surgery, Sivas Cumhuriyet University Faculty of Medicine, Sivas, Türkiye

## ABSTRACT

**Objective:** This study investigates the effects of adipose tissue-derived mesenchymal stem cell (MSC), human recombinant epidermal growth factor (EGF) and silver sulfadiazine (SSD) on wound healing in the burn stasis zone by applying the comb burn model in rats.

**Material and Methods:** A comb burn model was used for the burns and 32 Wistar albino female rats were randomly divided into four groups (control, SSD, SSD+MSC, SSD+EGF). On the 1<sup>st</sup> day and the 21<sup>st</sup> day, the total burn area on the 1<sup>st</sup> day and the healed, healing, and non-healing burn area on the 21<sup>st</sup> day were calculated with the Image-J program. At the end of the 21<sup>st</sup> day, the pathology samples taken after euthanasia were scored semiquantitatively in terms of epithelization, inflammatory cell density, fibroblast density, collagen amount, and angiogenesis after hematoxylin-eosin staining.

**Results:** Histopathological analysis demonstrated that epithelialization scores were highest in the MSC ( $3.88 \pm 0.35$ ,  $p < 0.001$ ) and EGF ( $3.63 \pm 0.52$ ) groups, while the control group had the lowest values ( $1.50 \pm 0.53$ ). Inflammatory cell density was significantly lower in the MSC ( $1.50 \pm 0.53$ ,  $p < 0.001$ ) and EGF ( $1.88 \pm 0.64$ ) groups than in the control group ( $3.75 \pm 0.46$ ). Similarly, fibroblast density was lowest in the MSC ( $1.38 \pm 0.52$ ,  $p < 0.001$ ) and EGF ( $1.75 \pm 0.71$ ) groups, while the control group had the highest values ( $3.63 \pm 0.52$ ). Collagen fibril density was significantly increased in the MSC ( $3.88 \pm 0.35$ ,  $p < 0.001$ ) and EGF ( $3.50 \pm 0.53$ ) groups compared to the control ( $1.63 \pm 0.74$ ). Angiogenesis was highest in the EGF group ( $3.75 \pm 0.46$ ,  $p < 0.001$ ), followed by the MSC group ( $3.00 \pm 0.53$ ), while the control group had the lowest values ( $1.25 \pm 0.46$ ). These results suggest that MSC and EGF play a significant role in wound healing, with MSC demonstrating superior epithelialization and EGF exhibiting the greatest angiogenic effect. Photo-analytical measurements showed that on day 1, burn area sizes were similar among all groups ( $p > 0.05$ ). By day 21, the healing burn area was significantly smaller in the MSC ( $3.19 \pm 0.98$  cm<sup>2</sup>,  $p < 0.001$ ) and EGF ( $4.33 \pm 0.48$  cm<sup>2</sup>) groups compared to the control ( $8.43 \pm 2.35$  cm<sup>2</sup>). The non-healing area was smallest in the EGF group ( $0.67 \pm 0.49$  cm<sup>2</sup>), followed by the MSC ( $1.06 \pm 0.49$  cm<sup>2</sup>,  $p < 0.001$ ) and SSD ( $1.91 \pm 0.75$  cm<sup>2</sup>) groups, whereas the control group had the largest non-healing area ( $7.29 \pm 2.20$  cm<sup>2</sup>). These findings suggest that MSC was the most effective treatment for promoting wound healing, followed by EGF and SSD.

**Conclusion:** We determined that both histologically and photo analytically, MSC and EGF provided faster wound healing in the burn stasis zone EGF gave better results than all groups in preventing necrosis.

**Keywords:** Burn, burn stasis zone, silver sulfadiazine, epidermal growth factor, mesenchymal stem cell

## INTRODUCTION

Burn injuries remain a major clinical challenge, leading to significant morbidity and mortality worldwide (1). Current burn treatments primarily focus on infection control and symptom management rather than active tissue regeneration, leading to suboptimal outcomes in preventing tissue loss (2).

Among the three burn wound zones, the stasis zone is particularly critical due to its potential for tissue salvage. Without appropriate intervention, this area may progress to necrosis, making it a key target for burn treatment (3-5).

Conventional treatments have limited effectiveness in preventing tissue loss in the stasis zone. One of the most widely used topical agents in burn treatment is silver sulfadiazine (SSD), but SSD does not actively support tissue regeneration (6). Mesenchymal stem cells (MSCs) and epidermal growth factor (EGF) have shown promising results in wound healing. MSCs have been shown to accelerate wound healing, improve angiogenesis, shape the extracellular matrix (ECM) while inhibiting the inflammatory response and promote cutaneous wound healing (7-10). EGF contributes to wound healing by enhancing cellular proliferation and migration, promoting angiogenesis, regulating inflammation, and supporting the remodeling of the ECM (11-13).

**Cite this article as:** Kürklü Ö, Soylu S. Comparison of the effects of epidermal growth factor mesenchymal stem cell and silver sulfadiazine on burn stasis zone. *Turk J Surg.* 2025;41(2):135-140

### Corresponding Author

Ömer Kürklü

E-mail: omerkurklu@gmail.com

ORCID ID: orcid.org/0000-0003-4770-1317

Received: 15.12.2024

Accepted: 05.03.2025

Epub: 19.03.2025

Publication Date: 30.05.2025

DOI: 10.47717/turkjsurg.2025.6684

Available at [www.turkjsurg.com](http://www.turkjsurg.com)



While MSCs and EGF have been studied in general wound healing, no prior study has systematically evaluated their direct effects in the burn stasis zone. By addressing this gap, our study provides critical insights into their potential for preserving tissue viability in burn injuries. We hypothesize that MSC and EGF treatments will significantly enhance tissue regeneration in the burn stasis zone by reducing inflammation, promoting epithelialization, and increasing angiogenesis compared to standard treatment. This study investigated the curative effects of adipose tissue-derived allogeneic MSCs and human recombinant EGF on the rat "burn stasis zone" by creating an experimental Comb burn model.

## MATERIAL and METHODS

### Ethical Approval and Animal Model

All animals used in this study were obtained from Sivas Cumhuriyet University Experimental Research Center, and all experimental procedures were approved by the Sivas Cumhuriyet University Ethics Committee (approval number: 65202830-050.04.04-351, date: 16.01.2020). All procedures complied with the Sivas Cumhuriyet University Experimental Animals Ethics Directive, which aligns with the Universal Declaration of Animal Rights, the European Convention for the Protection of Vertebrate Animals used for Experimental and Other Scientific Purposes (European

Treaty Series-no.123), the National Research Council of the USA, the United Nations Convention on International Trade in Endangered Species of wild fauna and flora (CITES), and the Bern Convention. This study also adheres to the animal research: Reporting of *in vivo* experiments guidelines (14). All procedures were performed under the supervision of a veterinarian.

Thirty-two female Wistar albino rats (200-250 g) were housed in a temperature-controlled environment (22-24 °C) with ad libitum access to food and water. The animals were randomly divided into four equal groups (n=8 per group). Euthanasia was performed on the 21<sup>st</sup> day using an overdose of pentothal sodium (200 mg/kg), and tissue samples were collected for analysis.

### Burn Wound Model

The burn wounds were created based on an established comb burn model. The rats were anesthetized with an intraperitoneal injection of xylazine (10 mg/kg) and ketamine (40 mg/kg). After shaving the dorsal skin, the area was disinfected with povidone-iodine. A metal comb, heated in boiling water (100 °C) for three minutes, was applied perpendicularly to the dorsal skin for 30 seconds without exerting pressure to induce a second-degree burn. (Figure 1A-C). The depth of the burn injury was histopathologically confirmed (15).

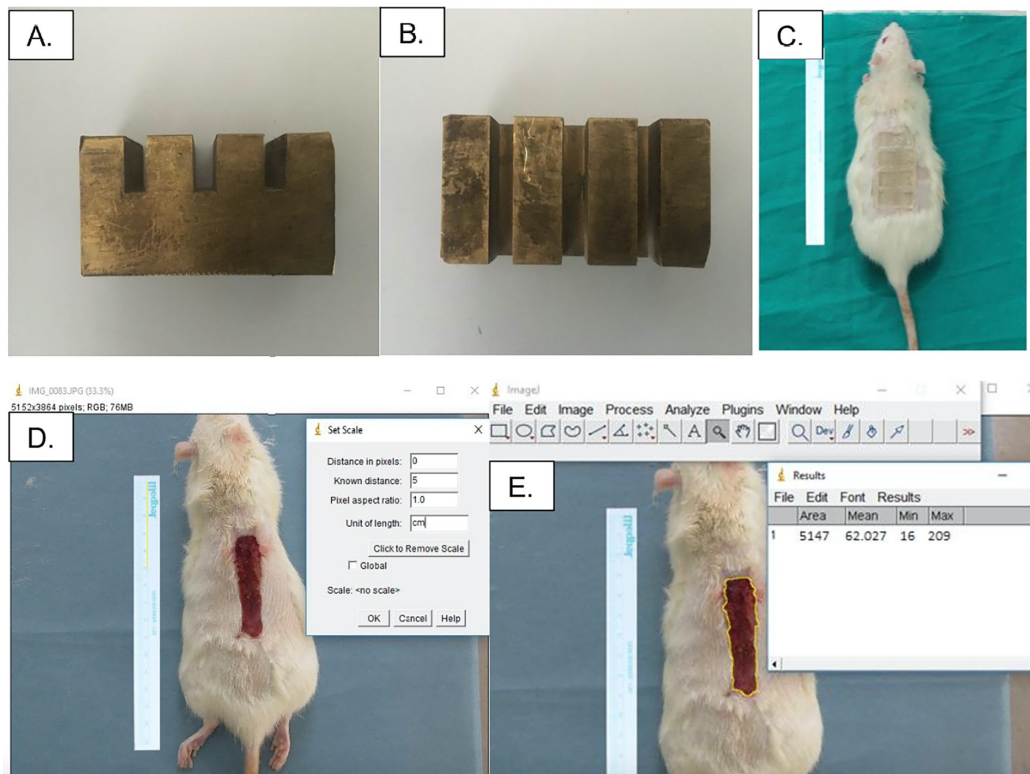


**Figure 1.** Creating a burn model with the comb and photo analysis of burnt areas. A, B. Brass plate prepared in accordance with the Comb burn model. C. The image created after the burn was made. D. Calibration was performed with the ImageJ program. E. The total burn surface area measurement on day 21 of a rat from the treatment groups was performed as an example using the ImageJ program.

## Experimental Groups and Treatment Protocols

The animals were divided into four groups:

- **Control group (n=8):** No treatment was applied after burn injury.
- **SSD group (n=8):** SSD (Silverdin) was applied epidermally to the stasis zone once daily for 21 days.
- **MSC group (n=8):** Adipose-derived MSCs were injected subcutaneously into the stasis zone on days 1, 3, 7, and 14; and SSD was applied epidermally daily.
- **EGF group (n=8):** Reconstituted lyophilized recombinant EGF (75 µg) was injected intradermally into the stasis zone on days 1, 3, 7, and 14; and SSD was applied epidermally daily.

## MSC Isolation and Culture

Adipose-derived MSCs were prepared at Kocaeli University Stem Cell and Gene Therapies Research Center following the protocol by Konno et al. (16).

- **Tissue source:** Adipose tissue was harvested from healthy Wistar rats via surgical excision under sterile conditions.
- **Isolation:** The tissue was digested with 0.1% collagenase type I for 45 minutes at 37 °C. The resulting cell suspension was filtered and centrifuged at 1.500 rpm for 10 minutes.
- **Culture conditions:** Cells were cultured in Dulbecco's modified eagle medium supplemented with 10% fetal bovine serum (FBS) and 1% penicillin/streptomycin at 37 °C with 5% CO<sub>2</sub>.
- **Passage and expansion:** Cells were expanded until 80-90% confluence and passaged using trypsin. Passage numbers 2 to 3 of cells were used for the experiment.
- **Injection protocol:** Each rat received 100,000 MSCs (1×10<sup>5</sup> cells) diluted in 100 µL PBS, injected subcutaneously at four points 0.5 cm from the burn stasis zone on days 1, 3, 7, and 14.

## EGF Preparation and Administration

A lyophilized recombinant EGF (75 µg) was reconstituted in 1 mL sterile saline. The solution was intradermally injected at four points within the stasis zone on days 1, 3, 7, and 14 using

a 30 G insulin syringe. The total injected volume was 0.1 mL per injection site per rat.

## Photoanalysis of Burn Areas

Photographs were taken on days 1 and 21 with a standardized distance of 50 cm and a guide ruler. Image analysis was performed using ImageJ software, and total burn area (cm<sup>2</sup>) and non-healing area (coagulation necrosis) were calculated separately (Figure 1D, E).

## Histopathological Evaluation

At the end of the study, rats were sacrificed using CO<sub>2</sub> inhalation euthanasia. The epidermis, dermis, adjacent healthy skin, and wound area were excised and fixed in 10% neutral buffered formalin for 48 hours. The tissues were processed with graded ethanol (70%, 80%, 96%, 100%) and embedded in paraffin. 5-µm-thick sections were obtained using a Leica RM2245 microtome. Hematoxylin-eosin staining was performed, and the samples were evaluated under a light microscope (Olympus BX51).

A semi-quantitative scoring system was used to assess epithelialization, inflammatory cell density, fibroblast cell density, collagen fibril density, and angiogenesis (Table 1).

## Statistical Analysis

Statistical analyses were performed using GraphPad Prism. Two-Way analysis of variance (ANOVA) was used for repeated measures in the same group over time (burn area changes between days 1 and 21). One-Way ANOVA followed by Tukey's post hoc test was used for comparisons between groups. The Kruskal-Wallis test was applied for non-parametric data. A power analysis was conducted using G\*Power software to determine the minimum sample size required for a power of 0.8 and α=0.05.

## RESULTS

### Histopathological Evaluation

Sections taken from the groups were stained with hematoxylin-eosin. The tissues of all groups were examined under the light microscope and evaluated by semi-quantitative scoring. Significant morphological damage was observed in the

**Table 1.** Semi-quantitative scoring of the tissue samples

Epithelialization	Inflamatur cell density	Fibroblast cell density	Collogen fiber density	Angiogenesis
0: None	0: None	0: None	0: None	0: Very rare formation of new vessels
1: Epithelialization 30%	1: A few inflamatur cells	1: A few fibroblast cells	1: A few collogen fibers	1: Rare formation of new vessels
2: Epithelialization 30-50%	2: Medium level inflamatur cell density	2: Medium level fibroblast cell density	2: Medium level collogen fiber density	2: Medium level formation of new vessels
3: Epithelialization 50-85%	3: Lots of inflamatur cell density	3: Lost of fibroblast cell density	3: Lots of collogen fiber density	3: Numereus formation of new vessels
4: Epithelialization 85-100%	4: High level inflamatur cell density	4: High level fibroblast cell density	4: High level collogen fiber density	4: Intense formation of new vessels

epithelial tissue of the control group (Figure 2A-A'). When the treatment groups were examined, it was observed that the epithelialization improved morphologically in the MSC, EGF, and SSD groups compared to the control group (Figure 2B-B', C-C', D-D'). In the control group, it was observed that the number of inflammatory cells due to the burn wound was quite high (Figure 2A-A'). Inflammatory cell density was significantly reduced in the EGF and SSD groups compared to the control group (Figure 2B-B', D-D'). The group with the least number of inflammatory cells was identified as the MSC group (Figure 2C-C'). It was determined that fibroblast cell density was quite high in the control group and gradually decreased in the treatment groups, (MSC, EGF, and SSD in order of fibroblast cell density from low to high). Collagen fibrils were determined most intensely in the control group and decreased in the SSD, EGF, and MSC groups, respectively. Angiogenesis, from the lowest to the highest among the groups, respectively; EGF, MSC, SSD, and control group (Figure 2A-A', B-B', C-C', D-D').

#### Comparison of Histopathological Data According to Experimental Groups

In the analysis of histopathological data, it was determined that there was a statistically significant difference between the groups. At the end of the 21<sup>st</sup> day, the experimental groups were evaluated in terms of epithelialization, inflammatory

cell density, fibroblast cell density, collagen fibrous density, and angiogenesis, which we determined as histopathological parameters. Inflammatory cell density was higher in the control group. However, inflammatory cell density was significantly decreased in the MSC and EGF group compared to the control group (\*\* $p < 0.01$ , \*\*\*\* $p < 0.0001$ ) (Figure 3A). Fibroblast cell density was higher in the control group. However, fibroblast cell density was significantly reduced in the MSC and EGF groups compared to the control group. However, fibroblast cell density detected in MSC and EGF groups was also found to be significantly lower than in the SSD group (\*\* $p < 0.01$ , \*\*\*\* $p < 0.0001$ ) (Figure 3B). Angiogenesis rates were compared between the groups. Angiogenesis was significantly increased in MSC and EGF groups compared to control and SSD groups (\*\* $p < 0.01$ , \*\*\* $p < 0.001$ , \*\*\*\* $p < 0.0001$ ) (Figure 3C). Collagen fibril density was found to be significantly lower in the control group compared to the other groups. Collagen fibril density was significantly increased in the MSC and EGF groups compared to the control and SSD groups (\*\* $p < 0.01$ , \*\*\*\* $p < 0.0001$ ) (Figure 3D).

The group with the best epithelialization recovery was the MSC group. Similarly, epithelialization was significantly higher in the EGF group than in the control group (\* $p < 0.1$ , \*\* $p < 0.01$ ) (Figure 3E).

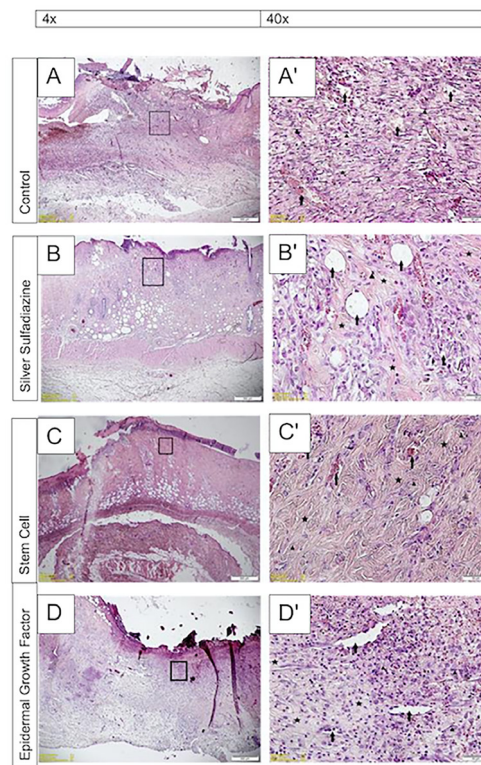


**Figure 2.** Morphological images for control and treatment groups. All specimens were investigated at 4x and 40x magnification with hematoxylin eosin under the light microscope. Sections from A-A': control group, B-B': Silver sulfadiazine group, C-C': Stem cell group, and D-D': Epidermal growth factor group. Blood vessels are indicated by the black arrow; collagen fibers are indicated by stars; fibroblasts are indicated by the arrowhead.



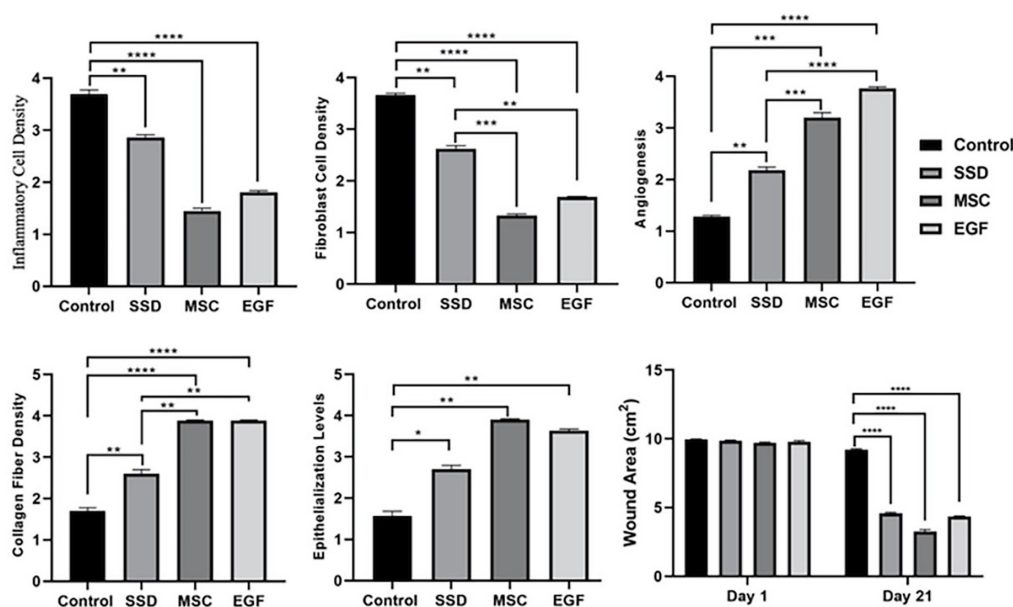


**Figure 3.** Comparison of epithelialization levels, inflammatory cell density levels, fibroblast cell density levels, collagen fiber density levels, angiogenesis levels, wound area, and non-healing area of experimental groups. (\* $p<0.1$ , \*\* $p<0.01$ , \*\*\* $p<0.001$ , \*\*\*\* $p<0.0001$ ).

Using the photo analytical results, the one-day burn area and the 21-day burn area were calculated. In addition, at the end of the 21<sup>st</sup> day, the non-healing area in the burn area with irregular wound healing and necrosis was calculated. For calculations, photographs were taken from a distance of 50 cm using a guide ruler, and the ImageJ program was utilized. The groups were evaluated in terms of burn area on the first day. It was determined that the created burn area was not significantly different between the groups. Burn areas where healing continued on the 21<sup>st</sup> day were compared. It was observed that the area in the SSD, MSC, and EGF groups, was significantly reduced compared to the control group, (\*\*\*\* $p<0.0001$ ) (Figure 3F).

On the 21<sup>st</sup> day, the groups were compared in terms of regular healing in the burn area, areas without regular epithelialization, and areas with necrosis. The non-healing area was found to be significantly smaller in the SSD, MSC, and EGF groups compared to the control group (\*\* $p<0.01$ , \*\*\* $p<0.001$ , \*\*\*\* $p<0.0001$ ) (Figure 3F).

## DISCUSSION

This study is one of the first to compare the effects of MSCs and EGF on the burn stasis zone. Our results demonstrate that MSCs are more effective in promoting epithelialization, while EGF is superior in preventing necrosis. These findings suggest that MSCs and EGF have distinct but complementary roles in burn wound healing.

Burn wound progression significantly impacts morbidity by increasing necrosis, infection risk, and the need for surgical interventions. Our results indicate that intradermal EGF

administration significantly reduced necrotic areas, whereas MSCs contributed more to epithelialization. These findings support the potential therapeutic role of MSCs and EGF in burn treatment.

Although MSC therapy has been widely studied in burn healing, no prior research has specifically evaluated the effects of subcutaneous adipose-derived MSC injection on the burn stasis zone. Consistent with previous findings, our results suggest that MSCs promote vascularization, reduce oxidative stress, and enhance tissue repair (17-21). EGF, a well-known mitogenic factor, demonstrated a significant reduction in necrosis, likely through its pro-angiogenic effects (22). However, MSCs exhibited broader paracrine activity, potentially explaining their greater impact on epithelialization.

## Study Limitations

This study was conducted in a rat model, and further clinical studies are required to determine its applicability in human patients. The small sample size, lack of standardized dosing, and absence of a combined MSC-EGF treatment group are limitations. Additionally, the long-term effects of MSC and EGF remain unknown.

## CONCLUSION

Given these findings, MSCs and EGF may offer promising therapeutic options for severe burns. Their ability to prevent burn wound progression could reduce infection risk, limit the need for debridement and grafting, and improve functional and cosmetic outcomes in burn patients. Future studies should focus on optimizing treatment protocols, evaluating combination

therapies, and conducting clinical trials to establish their role in standard burn care.

### Ethics

**Ethics Committee Approval:** All animals used in this study were obtained from Sivas Cumhuriyet University Experimental Research Center, and all experimental procedures were approved by the Sivas Cumhuriyet University Ethics Committee (approval number: 65202830-050.04.04-351, date: 16.01.2020).

**Informed Consent:** As this study involves animals, consent is not required.

### Footnotes

#### Author Contributions

Conception - S.S.; Design - S.S.; Supervision - S.S.; Data Collection and/or Processing - Ö.K.; Analysis and/or Interpretation - S.S., Ö.K.; Literature Review - Ö.K.; Writer - Ö.K.; Critical Review - S.S., Ö.K.

**Conflict of Interest:** No conflict of interest was declared by the authors.

**Financial Disclosure:** The authors declared that this study received no financial support.

### REFERENCES

- Wang M, Xu X, Lei X, Tan J, Xie H. Mesenchymal stem cell-based therapy for burn wound healing. *Burns Trauma*. 2021;9:tkab002.
- Magne B, Lataillade JJ, Trouillas M. Mesenchymal stromal cell preconditioning: The next step toward a customized treatment for severe burn. *Stem Cells Dev*. 2018;27:1385-1405.
- Jackson DM. [The diagnosis of the depth of burning]. *Br J Surg*. 1953;40:588-596.
- Mahajan AL, Tenorio X, Pepper MS, Baetens D, Montandon D, Schlaudraff KU, et al. Progressive tissue injury in burns is reduced by rNAPc2. *Burns*. 2006;32:957-963.
- Hettiaratchy S, Dziewulski P. ABC of burns: pathophysiology and types of burns. *BMJ*. 2004;328:1427-1429. Erratum in: *BMJ*. 2004;329:148.
- Warriner R, Burrell R. Infection and the chronic wound: a focus on silver. *Adv Skin Wound Care*. 2005;18(Suppl 1):2-12.
- Walter MN, Wright KT, Fuller HR, MacNeil S, Johnson WE. Mesenchymal stem cell-conditioned medium accelerates skin wound healing: an in vitro study of fibroblast and keratinocyte scratch assays. *Exp Cell Res*. 2010;316:1271-1281.
- Maharlooei MK, Bagheri M, Solhjoui Z, Jahromi BM, Akrami M, Rohani L, et al. Adipose tissue derived mesenchymal stem cell (AD-MSC) promotes skin wound healing in diabetic rats. *Diabetes Res Clin Pract*. 2011;93:228-234.
- Nie C, Yang D, Xu J, Si Z, Jin X, Zhang J. Locally administered adipose-derived stem cells accelerate wound healing through differentiation and vasculogenesis. *Cell Transplant*. 2011;20:205-216.
- Zhang QZ, Su WR, Shi SH, Wilder-Smith P, Xiang AP, Wong A, et al. Human gingiva-derived mesenchymal stem cells elicit polarization of m<sup>2</sup> macrophages and enhance cutaneous wound healing. *Stem Cells*. 2010;28:1856-1868.
- Zhao R, Liang H, Clarke E, Jackson C, Xue M. Inflammation in chronic wounds. *Int J Mol Sci*. 2016;17:2085.
- Kamińska A, Enguita FJ, Stępień EL. Lactadherin: An unappreciated haemostasis regulator and potential therapeutic agent. *Vascul Pharmacol*. 2018;101:21-28.
- Hardwicke J, Schmaljohann D, Boyce D, Thomas D. Epidermal growth factor therapy and wound healing-past, present and future perspectives. *Surgeon*. 2008;6:172-177.
- Percie du Sert N, Hurst V, Ahluwalia A, Alam S, Avey MT, Baker M, et al. The ARRIVE guidelines 2.0: Updated guidelines for reporting animal research. *PLoS Biol*. 2020;18:e3000410.
- Oryan A, Alemzadeh E, Moshiri A. Burn wound healing: present concepts, treatment strategies and future directions. *J Wound Care*. 2017;26:5-19.
- Konno M, Hamabe A, Hasegawa S, Ogawa H, Fukusumi T, Nishikawa S, et al. Adipose-derived mesenchymal stem cells and regenerative medicine. *Dev Growth Differ*. 2013;55:309-318.
- Yi H, Wang Y, Yang Z, Xie Z. Efficacy assessment of mesenchymal stem cell transplantation for burn wounds in animals: a systematic review. *Stem Cell Res Ther*. 2020;11:372.
- Chang YW, Wu YC, Huang SH, Wang HD, Kuo YR, Lee SS. Autologous and not allogeneic adipose-derived stem cells improve acute burn wound healing. *PLoS One*. 2018;13:e0197744. Erratum in: *PLoS One*. 2020;15:e0238935.
- Schneider I, Calcagni M, Buschmann J. Adipose-derived stem cells applied in skin diseases, wound healing and skin defects: a review. *Cytotherapy*. 2023;25:105-119.
- Bliley JM, Argenta A, Satish L, McLaughlin MM, Dees A, Tompkins-Rhoades C, et al. Administration of adipose-derived stem cells enhances vascularity, induces collagen deposition, and dermal adipogenesis in burn wounds. *Burns*. 2016;42:1212-1222.
- Abbas OL, Özatik O, Gönen ZB, Ögüt S, Özatik FY, Salkın H, et al. Comparative analysis of mesenchymal stem cells from bone marrow, adipose tissue, and dental pulp as sources of cell therapy for zone of stasis burns. *J Invest Surg*. 2019;32:477-490.
- Ching YH, Sutton TL, Pierpont YN, Robson MC, Payne WG. The use of growth factors and other humoral agents to accelerate and enhance burn wound healing. *Eplasty*. 2011;11:e41.